Journal of Cerebral Blood Flow & Metabolism (2014) 34, 1128–1137

www.jcbfm.com

ORIGINAL ARTICLE

Medullary norepinephrine neurons modulate local oxygen concentrations in the bed nucleus of the stria terminalis

Elizabeth S Bucher, Megan E Fox, Laura Kim, Douglas C Kirkpatrick, Nathan T Rodeberg, Anna M Belle and R Mark Wightman

Neurovascular coupling is understood to be the underlying mechanism of functional hyperemia, but the actions of the neurotransmitters involved are not well characterized. Here we investigate the local role of the neurotransmitter norepinephrine in the ventral bed nucleus of the stria terminalis (vBNST) of the anesthetized rat by measuring O_2, which is delivered during functional hyperemia. Extracellular changes in norepinephrine and O_2 were simultaneously monitored using fast-scan cyclic voltammetry. Introduction of norepinephrine by electrical stimulation of the ventral noradrenergic bundle or by iontophoretic ejection induced an initial increase in O_2 levels followed by a brief dip below baseline. Supporting the role of a hyperemic response, the O_2 increases were absent in a brain slice containing the vBNST. Administration of selective pharmacological agents demonstrated that both phases of this response involve β-adrenoceptor activation, where the delayed decrease in O_2 is sensitive to both α- and β-receptor subtypes. Selective lesioning of the locus coeruleus with the neurotoxin DSP-4 confirmed that these responses are caused by the noradrenergic cells originating in the nucleus of the solitary tract and A1 cell groups. Overall, these results support that non-coerulean norepinephrine release can mediate activity-induced O_2 influx in a deep brain region.

Journal of Cerebral Blood Flow & Metabolism (2014) **34,** 1128–1137; doi:10.1038/jcbfm.2014.60; published online 9 April 2014

Keywords: neurochemistry; neurotransmitters; neurovascular coupling; pharmacology; receptors

INTRODUCTION

The neurovascular unit, composed of neuronal, glial, and vascular elements, serves to support brain function by matching O_2-rich blood flow with the metabolic demands of regional activity. It is understood that the products of local neurotransmission trigger this response, known as functional hyperemia; however, much remains to be learned regarding the actions and mechanisms of the chemical messengers involved.[1] This information is crucial to understanding disease pathologies that involve dysregulation of cerebral blood flow (CBF)—including cerebral ischemia[2] and many forms of dementia[3]—as well as to interpreting data from brain imaging techniques such as blood O_2 level-dependent functional magnetic resonance imaging.

The catecholamine norepinephrine is one major neurotransmitter implicated in this hemodynamic process. Its neurons lie in several nuclei, designated A1 to 7, scattered along the hindbrain and brainstem. These cell populations diffusely project throughout the brain and terminate primarily as non-junctional varicosities,[4] allowing their activity to exert a broad field of influence. The noradrenergic neurons of the locus coeruleus (LC, A6) are typically associated with the neurovascular unit. These neurons provide the majority of cortical noradrenergic input, and they terminate proximal to both astrocytes and microvessels.[5,6] The presence of adrenoceptors on these neurovascular targets,[7] which are sensitive to LC denervation,[5,8] provides further evidence that the LC norepinephrine system is positioned to influence their activities. Indeed, studies have established that noradrenergic signaling can influence energy metabolism,[9] vascular permeability,[10] ionic fluctuations in astrocytes,[11] as well as glutamate signaling by modulation of its synthesis[12] and uptake.[13] Other reports have demonstrated that CBF responses coincide with altered LC activity.[10,14,15]

Here we consider the vasoactivity of norepinephrine in a region weakly innervated by the LC: the ventral bed nucleus of the stria terminalis (vBNST). The vBNST is a structure of the extended amygdala involved in the autonomic and behavioral responses to stress.[16] We targeted this deep brain region as it receives the densest norepinephrine input in the brain.[17] Its noradrenergic innervation arises primarily from the nucleus of the solitary tract (A2) and the A1 cell group through the ventral noradrenergic bundle (VNB).[18] These cell groups are located in the medulla oblongata, and receive cardiovascular, respiratory, gastrointestinal, and other visceral information from peripheral afferents. Although these norepinephrine populations have not been formally associated with cerebral hemodynamic function, their terminals are associated with the perivascular space in regions such as the paraventricular nucleus.[19] In addition, non-specific chemical stimulation of nucleus of the solitary tract neurons attenuates CBF, and this effect is believed to be neurogenic in origin.[20]

In this study, norepinephrine concentrations were transiently increased within the vBNST by electrical stimulation of the VNB and by local application through iontophoresis. Fast-scan cyclic voltammetry at a carbon fiber microelectrode was employed to simultaneously detect norepinephrine transients and changes in extracellular O_2 with subsecond and micrometer resolution. Extracellular O_2 is a function of ongoing metabolism and local blood flow. We found that surges of norepinephrine in the vBNST are accompanied by an increase in O_2 that is followed by a transient decrease below baseline levels. This response is due to the local actions of norepinephrine at its receptors and does not

Department of Chemistry and Neuroscience Center, University of North Carolina at Chapel Hill, Chapel Hill, North Carolina, USA. Correspondence: Dr RM Wightman, Department of Chemistry, Campus Box 3290, Caudill and Kenan Laboratories, The University of North Carolina at Chapel Hill, Chapel Hill, NC 27599, USA.
E-mail: rmw@unc.edu

This work was funded by NIH grant to RMW (DA32530). ESB was supported by a fellowship from Eastman Chemical Company.
Received 5 September 2013; revised 20 February 2014; accepted 3 March 2014; published online 9 April 2014

depend on LC functionality. In a brain slice that lacks CBF, iontophoresis of norepinephrine had no effect on measured O_2 concentrations whereas electrical stimulation caused O_2 concentration to decrease, supporting a role for functional hyperemia as the origin of our *in vivo* results.

MATERIALS AND METHODS

Chemicals and Drugs

All chemicals and drugs were used as received from Sigma-Aldrich (St Louis, MO, USA), unless otherwise noted.

Electrode Fabrication

Two electrode types were employed in this study. Experiments without iontophoresis used single barrel carbon fiber microelectrodes.[21] Each electrode was cut under a light microscope to an exposed length of 100 μm. For iontophoresis experiments, voltammetric recordings were made with four-barrel probes.[22] One barrel housed a carbon fiber electrode while the other three barrels contained the desired solutions.

Fast-Scan Cyclic Voltammetry

Fast-scan cyclic voltammetry was computer controlled using a data acquisition program (High Definition Cyclic Voltammetry, UNC-Chapel Hill, NC, USA)[23] programmed in LabVIEW (National Instruments, Austin, TX, USA). A single PCIe-6363 card (National Instruments) generated the voltammetric and stimulation waveforms and simultaneously collected cyclic voltammograms. The voltammetric waveform was applied to the carbon fiber microelectrode and its current response transduced through a locally constructed UEI potentiostat (UNC Department of Chemistry Electronics Design Facility).

Voltammetric recordings employed two waveforms. For electrode placement, iontophoresis barrel priming, and post-experiment signal verification, a triangular waveform designed specifically for catecholamine detection was used. This waveform scanned between -0.4 and 1.3 V at 400 V/second.[24] For combined measurements of O_2 and norepinephrine, the voltage ramp scanned at 400 V/second between 0.8 and -1.4 V with a holding potential of 0 V.[25] Before use of either waveform, the electrode was conditioned with the voltage ramp for 15 minutes at 60 Hz and 15 minutes at 10 Hz. Recordings were made at a 10 Hz application frequency.

Calibrations

Electrode responses to norepinephrine, O_2, and 4-methylcatecholamine were determined through an air-impermeable flow-injection analysis system with glass syringes and PEEK tubing (Sigma-Aldrich). All standards were prepared in Tris buffer (15 mmol/L Tris, 126 mmol/L NaCl, 2.5 mmol/L KCl, 25 mmol/L $NaHCO_3$, 2.4 mmol/L $CaCl_2$, 1.2 mmol/L NaH_2PO_4, 1.2 mmol/L $MgCl_2$, 2.0 mmol/L Na_2SO_4) adjusted to pH 7.4 with NaOH. O_2 calibrations employed a N_2-purged solution, an air-saturated solution, and an O_2-saturated solution. Peak reduction currents were taken for O_2 calibrations, while peak oxidation currents were used for the catecholamines. The average calibration factors were as follows: 16.4 nA/μmol/L norepinephrine ($+1.3$ V waveform), -0.3 nA/μmol/L O_2 and 8.9 nA/μmol/L 4-methylcatechol (O_2-sensitive waveform).

Voltammetric Data Presentation and Analysis

Fast-scan cyclic voltammetry data were processed through the High Definition Cyclic Voltammetry analysis program. Each file was digitally filtered (4th order low pass Bessel, 2 KHz cutoff) and background subtracted from baseline currents. Data are presented as color plots, with the waveform plotted along the ordinate and the acquisition time shown along the abscissa. Currents are mapped in false color in a 3: -2 ratio. Principal component regression, a multivariate chemometric algorithm, was used to determine concentrations for data collected on the -0.4 V/$+1.3$ V waveform.[26]

Unless otherwise indicated data are shown as mean ± s.e.m. All *n*-values represent number of animals. Data were considered statistically significant when $P<0.05$.

Surgery

All animal procedures were approved by the Institutional Animal Care and Use Committee of the University of North Carolina at Chapel Hill in accordance with the Public Health Service policy on Humane Care and Use of Laboratory Animals and the Amended Animal Welfare Act of 1985. Care was taken to minimize the number of animals used in this study and their suffering. Adult male Sprague–Dawley rats (300 to 400 g) were purchased from Charles River (Wilmington, MA, USA). Animals were anesthetized with urethane (1.5 g/kg) and placed in a stereotaxic frame (Kopf, Tujunga, CA, USA). Surgical procedures were as described previously[27] with anterior–posterior, medial–lateral, and dorsal–ventral coordinates referenced from bregma according to Paxinos and Watson (2007). A fresh carbon fiber microelectrode was lowered into the vBNST (anterior–posterior $+0.0$ mm, medial–lateral $+1.2$ mm, dorsal–ventral -7.0 to -7.8 mm), and an Ag/AgCl reference was implanted in the contralateral hemisphere. A bipolar stimulating electrode (Plastics One, West Lafayette, IN, USA) was placed in the VNB (anterior–posterior -5.2 mm, medial–lateral $+1.2$ mm, dorsal–ventral -8.0 to 8.6 mm) ipsilaterally to the recording electrode. Electrical stimulations (10 to 80 biphasic pulses, 60 Hz, ± 300 μA, 2 milliseconds per pulse) were delivered via an optically isolated stimulator (NL 800 A, Neurolog, Digitimer, Hertfordshire, UK). The depths of the carbon fiber and stimulating electrodes were adjusted to achieve maximal measured norepinephrine release.

In Vitro Procedure

Brain slices containing the vBNST were prepared from Sprague–Dawley rats (300 to 400 g) anesthetized with urethane (1.5 g/kg). Brains were quickly removed after decapitation and submerged in ice-cold, oxygenated (95% O_2/5% CO_2) bicarbonate buffer solution (87 mmol/L NaCl, 2.5 mmol/L KCl, 1.2 mmol/L NaH_2PO_4, 25 mmol/L $NaHCO_3$, 7 mmol/L $MgCl_2$, 0.5 mmol/L $CaCl_2$, 75 mmol/L sucrose) adjusted to pH 7.4. A Vibroslice NVSL Vibratome (World Precision Instruments, Sarasota, FL, USA) was used to cut 300 μm coronal sections. Bed nucleus of the stria terminalis slices were transferred to a perfusion chamber (RC-22, Warner Instruments, Hamden, CT, USA) fitted with a microscope (Eclipse FN-1 Fixed Stage Microscope, Nikon, Melville, NY, USA, Gibraltar Stage) and maintained under a flow (2 mL/minute) of oxygenated bicarbonate buffer (126 mmol/L NaCl, 2.5 mmol/L KCl, 1 mmol/L NaH_2PO_4, 26 mmol/L $NaHCO_3$, 1.2 mmol/L $MgCl_2$, 2.4 mmol/L $CaCl_2$, 11 mmol/L glucose) heated to 37 °C. For electrochemical recordings, a carbon fiber electrode was lowered 75 μm into the tissue underneath the anterior commissure. A tungsten bipolar stimulating electrode (Frederick Haer, Bowdoinham, ME, USA) was placed on the surface of the slice proximal to the recording electrode.

Pharmacological Investigations

In the first set of experiments, pharmacological agents were introduced systemically by intraperitoneal injection. First, a 30-minute baseline was established by repeating a 60 pulse electrical stimulus every 5 minutes. Next, sterile saline (1 mL) was administered as a vehicle control, followed by a selective norepinephrine drug. These included idazoxan (α_2 antagonist, 5 mg/kg), desipramine HCl (transporter inhibitor, 15 mg/kg), propranolol HCl (non-selective β-antagonist, 20 mg/kg), and terazosin (α_1 antagonist, 5 mg/kg, Tocris Bioscience, Bristol, UK). Doses were chosen to identify receptor contributions, not to quantitatively assess their relative effects. All drugs were dissolved in 0.5 mL saline, except for terazosin, which was dissolved in 1.0 mL saline with gentle heat. Data were collected for at least 45 minutes after drug administration to allow maximum effects.

A second set of experiments used iontophoresis to introduce the adrenoceptor antagonists as well as *N*-nitro-L-arginine methyl ester (L-NAME, nitric oxide (NO) synthase inhibitor) and 1-aminobenzotriazole (cytochrome P450 inhibitor, Tocris Bioscience) directly at the recording electrode. Iontophoresis solutions were prepared as 5 mmol/L drug, 5 mmol/L 4-methylcatechol, and 5 mmol/L NaCl, adjusted to pH 5.6. 4-methylcatechol provided an electroactive marker to monitor ejections with fast-scan cyclic voltammetry.[22] Drug concentrations were calculated from the relative mobility of each pharmacological agent relative to 4-methylcatechol. Ejections were induced by positive current (5 to 400 nA) generated by a constant current source (Neurophore, Harvard Apparatus, Holliston, MA, USA). Each iontophoresis barrel was primed at a depth dorsal to the vBNST (-5 mm to -6 mm) to ensure reproducible ejection profiles, and a negative retaining current (-1 to 10 nA) was applied to any leaking barrels. After baseline measurements were taken as described for the intraperitoneal protocol, drugs were applied through a 30-second

ejection. Ejection of 4-methylcatechol did not evoke O_2 changes (*vide infra*) and so it served as a control. Ejected drug concentrations were between 5 to 35 μmol/L at the carbon fiber. Measured ejections currents were allowed to return to baseline before stimulation data were collected.

A third type of pharmacological manipulation involved local introduction of norepinephrine-selective agonists through iontophoresis. Drugs were prepared as described for the antagonist ejections. Methoxamine ($\alpha_1$agonist) and clonidine (α_2 agonist) solutions contained 4-methylcatechol to monitor their ejections electrochemically. Norepinephrine and isoproterenol (non-selective β-agonist) were prepared without 4-methylcatechol as both are electroactive. Each was ejected in the vBNST for 1 second (3 to 5 minutes apart) to reproduce the duration of the electrical stimulation used in other portions of this study. Based on the capabilities of the iontophoresis barrel, a range of concentrations (between 1–20 μmol/L) was tested for each agonist. For some experiments antagonists were loaded into the remaining iontophoresis barrels. In these experiments, baseline norepinephrine responses were recorded for 30 minutes before an antagonist was administered following the protocol of the electrical stimulation experiments.

Signal Verification

The placement of the stimulating electrode also activates the dopaminergic neurons of the ventral tegmental area.[28] To ensure that the voltammetric catecholamine signal was due to norepinephrine, and not structurally-similar dopamine, each experiment ended with intraperitoneal administration of raclopride (dopamine D2 autoreceptor antagonist) followed by either idazoxan (α_2 autoreceptor antagonist) or desipramine (norepinephrine transporter inhibitor). Only locations that selectively responded to the norepinephrine drugs were used in this study.[28]

Histology

At the end of data collection, a constant potential (10 V, 30 seconds) was applied to the carbon fiber to lesion the recording site. Animals were then killed with an overdose of urethane. Brains were promptly removed and fixed with 10% formalin and post-fixed for at least three days before coronal slices (40 to 50 μm) were prepared on a freezing microtome (Leica, Wetzlar, Germany), mounted on a glass slide, coverslipped, and viewed under a light microscope.

Locus Coeruleus Lesioning with DSP-4

The LC-selective neurotoxin DSP-4 (N-(2-chloroethyl)-*N*-ethyl-2-bromobenzylamine)[29] was administered to rats ($n = 5$, 150 to 200 g) in two doses (0.5 mL, 50 mg/kg, intraperitoneal) 3 days apart. DSP-4 was dissolved in saline immediately before use. Measurements commenced 9 days after the last dose to allow peripheral effects to diminish. Untreated rats were used as a control in both experiments.

Immunohistochemistry

Rats were anaesthetized with urethane and transcardially perfused with 0.1 mol/L phosphate-buffered saline at pH 7.4, followed by 4% paraformaldehyde in phosphate-buffered saline. Brains were removed, post-fixed for >24 hours, then cryoprotected in 30% sucrose for >48 hours. Sections (40 μm) were cut with a freezing microtome (Leica) and collected in 0.1 mol/L phosphate-buffered saline.

Immunofluorescence procedures were adapted from elsewhere.[30] Briefly, sections were washed in 0.1 mol/L Tris-buffered saline (TBS), pH 7.4, then blocked with 5% normal donkey serum in TBS with 0.3% Triton X-100 (NDS-TBS-T) for 1 hour. Tissue was incubated overnight at 4 °C in primary cocktail prepared in NDS-TBS-T, which contained mouse anti glial fibrillary acidic protein (1:300, Sigma), rabbit-anti-DBH (1:500, Immunostar, Hudson, WI, USA), and biotinylated solanum tuberosum lectin (20 μg/mL, Vector). After 3 rinses in TBS-T, sections were incubated in secondary cocktail for 2 hours at room temperature. Secondary cocktail was prepared in TBS with 2% bovine serum albumin and contained AlexaFlour 488-conjugated goat-anti-rabbit immunoglobulin G (1:500, Life Technologies, Carlsbad, CA, USA), Alex Fluor 633-conjugated goat-anti-mouse immunoglobulin G (1:500, Life Technologies), and streptavidin-DyLight 405 (20 μg/mL, Fisher, Pittsburgh, PA, USA). Sections were rinsed extensively in TBS, mounted and coverslipped with Fluoromount (Sigma) before visualization on a confocal microscope.

Sections were analyzed with a FV1000 microscope (Olympus, Tokyo, Japan) equipped with a diode laser, argon laser, and helium-neon laser for the excitations of DyLight 405, Alexa Fluor 488, and Alexa Fluor 633, respectively. Images are based on a single optical section of <1 μm thickness, and captured using FV1000ASW software (Olympus). DBH quantification employed constant acquisition parameters and three sections (-0.05 mm to $+0.05$ mm anterior–posterior from bregma) were analyzed for each animal. Mean pixel intensity was analyzed using image J software in a 9000 square pixel area. For the vBNST, a rectangle of 450 by 200 pixels was drawn directly beneath the anterior commissure, and cortical sections were analyzed in a 300 by 300 pixel square.

Cardiorespiratory Measurements

The cardiorespiratory effects of anesthesia and systemic adrenergic antagonism were determined in a separate group of rats (300 to 400 g). A MouseOx pulse oximeter system equipped with a collar sensor (Starr Life Sciences, Oakmont, PA, USA) was used to monitor heart rate (beats per minute) and respiratory rate (breaths per minute). Pre-urethane measurements were taken with the animal at rest. Anesthetized data were collected 3 hours after administration of urethane (1.5 g/kg). Thereafter, one of four adrenergic antagonists (terazosin, idazoxan, propranolol or desipramine) was delivered (intraperitoneal) at the dose listed under *Pharmacological Investigations.* Post-drug cardiorespiratory values were recorded 35 minutes after injection.

RESULTS

Immunohistochemistry of Recording Environment

Immunohistochemistry was employed to provide an overview of the neurovascular environment of the vBNST on the spatial scale of our recording electrode. Three major neurovascular components were targeted: microvessels (STL), glial cells (glial fibrillary acidic protein), and norepinephrine terminals (DBH). Their distribution is shown in Figure 1. At these coordinates, the ventral portion of the BNST is located underneath the anterior commissure. A range of vessel sizes ($\sim$3 to 15 μm) were found within the vBNST confirming the presence of both arterioles and capillaries. Astrocytes were highly associated with the larger microvessels as well as with the myelinated axon fibers composing the anterior commissure.

Consistent with our previous work,[27] the densest region of noradrenergic innervation was located within the vBNST. At higher magnifications, these terminals appeared scattered within the perivascular space in proximity to both microvessels and astrocytes, as has been reported for cortical regions. Within the areas of highest terminal density, spanning only $\sim$1 mm along the medial–lateral plane, vascular heterogeneity is apparent. The dimensions of the carbon fiber microelectrode (100 μm length, 5 μm diameter, superimposed in Figure 1E) are small enough to probe these microenvironments. In these experiments, the placement of the carbon fiber electrode was optimized for the detection of norepinephrine, not for the detection of O_2 changes. Therefore, the immediate neurovascular landscape likely varied between recording locations.

O_2 Response with Electrical Stimulation

To investigate whether norepinephrine release in the vBNST coincides with O_2 changes, electrical stimulation of the VNB was used to induce norepinephrine overflow while extracellular O_2 and norepinephrine changes were monitored simultaneously. Norepinephrine has a peak oxidation potential of 0.75 V and a peak for reduction of its electroformed *o*-quinone at -0.2 V on the negative going scan. O_2 is reduced at -1.35 V on the negative going scan (Supplementary Figure 1). We found that O_2 changes accompanied VNB stimulation and that the responses were variable between animals (Supplementary Figure 2). Minor adjustment of the recording and stimulating electrode depths did not have a significant effect on the measured O_2 signal (Supplementary Figure 3). This suggests signal variability may be a result of anterior–posterior/medial–lateral positioning.

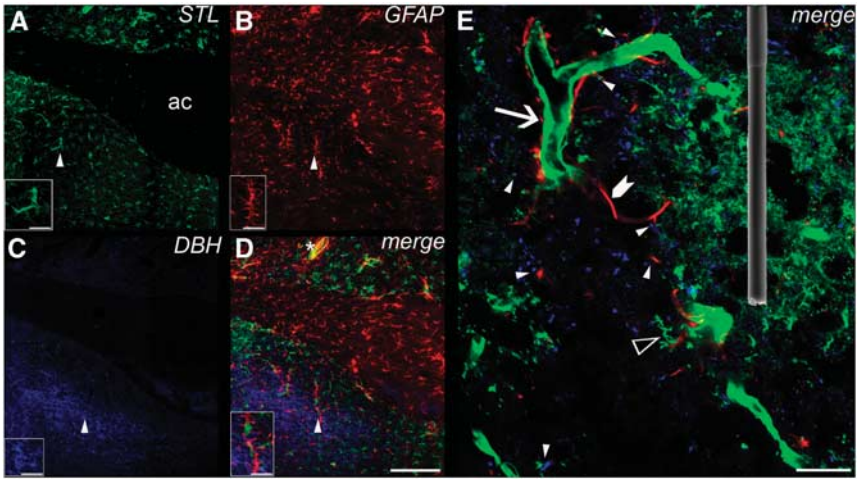

Figure 1. Confocal laser scanning images of triple-fluorescence labeling in the rat ventral bed nucleus of the stria terminalis (vBNST). (**A**) Lectin staining of vasculature and microglia with biotinylated Solanum tuberosum agglutinin (STL) and DyLight 405 conjugated streptavidin, color coded in green (AC, anterior commissure). Simultaneously labeled astroglia are shown in (**B**) with mouse anti-glial fibrillary acidic protein (GFAP) and Alexa Fluor-633-tagged goat anti-mouse immunoglobulin G (IgG), color coded in red. Concomitantly revealed norepinephrine terminals were color coded in blue, and visualized in (**C**) using rabbit anti-dopamine beta hydroxylase (DBH) and Alexa Fluor-488 goat anti-rabbit IgG. (**D**) A merge of **A**, **B**, and **C**. An example of glial vessel colocalization is indicated by an asterisk and appears yellow. Terminal glial colocalization is seen in pink. Scale bar, 200 μm. Insets demonstrate the triangle-labeled features at higher magnification. Scale bar, 50 μm. (**E**) Further magnification in a different slice revealed the diverse architecture of blood vessels (arrow), microglia (open triangle), astrocytes (chevron), and norepinephrine terminals (blue) within the vBNST. Sites where norepinephrine terminals interact with vessels and/or astroglia are indicated by closed triangles. An electron micrograph of a 100 μm long carbon fiber microelectrode is superimposed to demonstrate the electrochemical sampling environment. Scale bar, 20 μm.

One stimulated O_2 response predominated in our studies (~65% of locations) and thus was chosen for pharmacological characterization. In this response, O_2 levels rose after the stimulation and reached a maximum (6.98 ± 0.93 μmol/L) on average 1.9 ± 0.1 second after stimulation onset. This increase was subsequently followed by a transient dip below baseline concentrations (-3.98 ± 0.74 μmol/L), peaking 9.6 ± 0.2 seconds after the stimulation. We termed the initial O_2 increase as event 1 and the subsequent decrease as event 2. In many animals a second, prolonged increase in extracellular O_2 was measured after the initial response long after clearance of norepinephrine, similar to our previous recordings in the striatum.[25] The second O_2 increase was unaffected by local adrenoceptor pharmacology (Supplementary Figure 4). Thus, our discussion focuses on events 1 and 2.

Example data averaged over multiple trials from a single animal are provided in Figure 2A. Multiple chemical fluctuations are visible in the color plot. Immediately after the stimulation, norepinephrine release is apparent as positive current at its oxidation potential. Concurrent O_2 fluctuations appear at -1.35 V on the forward voltage scan. As O_2 is detected through its reduction, negative currents correspond to increases in concentration, while positive currents indicate decreases. These O_2 events are accompanied by pH changes[25] that overlap with the oxidation potential of norepinephrine at later times in the recording. A positive current feature occurs after the -1.4 V switching potential during the stimulation. It is because of adsorption of ions such as Ca^{2+}.[31]

The amplitude of each O_2 event was compared with the amount of released norepinephrine evoked by the electrical stimulation. While both responses correlated with peak norepinephrine concentration across animals, event 2 exhibited a better linear fit ($r^2 = 0.61$) in comparison to event 1 ($r^2 = 0.27$). To vary the amount of norepinephrine released in one location, the duration of the electrical stimulation was varied (0.17 to 1.33 seconds) by changing the number of electrical pulses applied. Norepinephrine release and the O_2 changes increased linearly with pulse number within this range. The response of event 1 to stimulation duration was significantly different from that of norepinephrine ($P < 0.01$) and of event 2 ($P < 0.05$). The pulse dependence of event 2, however, closely resembled the norepinephrine response ($P > 0.05$).

We also examined the effects of electrically stimulated norepinephrine release in a coronal brain slice that contained the vBNST. The stimulation (60 pulses, 60 Hz) was evoked with a bipolar electrode placed 100 to 200 μm from the carbon fiber electrode. After the stimulation, O_2 decreased by 36.1 ± 6.2 μmol/L in a monotonic fashion, reaching a minima 17.9 ± 3.1 second after the stimulation ($n = 3$ animals, two slices from each animal).

Effect of DSP-4 on Electrically Stimulated O_2 Response

To ascertain whether the stimulated O_2 changes were dependent on LC activity a subset of animals in this study was treated with the neurotoxin DSP-4. DSP-4 causes selective degradation of LC norepinephrine axons, leaving the norepinephrine neurons of the brainstem nuclei intact.[29] DSP-4 significantly reduced norepinephrine terminal density in the cortical region above the BNST ($P < 0.001$, $n = 5$), which receives its innervation solely from LC neurons.[29] DSP-4 did not, however, exert a significant effect on the terminal density within vBNST (Supplementary Figure 5). Responses to VNB stimulation also remained intact after DSP-4. In treated animals, no significant differences in peak times and magnitudes were found for norepinephrine release and the O_2 response (Table 1).

O_2 Response with Adrenoceptor Blockade

While electrical stimulation is an effective means to depolarize proximal neurons, its effects are relatively non-selective, causing release of other neuromodulators. We therefore employed selective antagonists to determine the involvement of noradrenergic receptors in the electrically stimulated O_2 response. Drugs were introduced both systemically (intraperitoneal injection) and locally at the recording site (iontophoresis ejection). Because

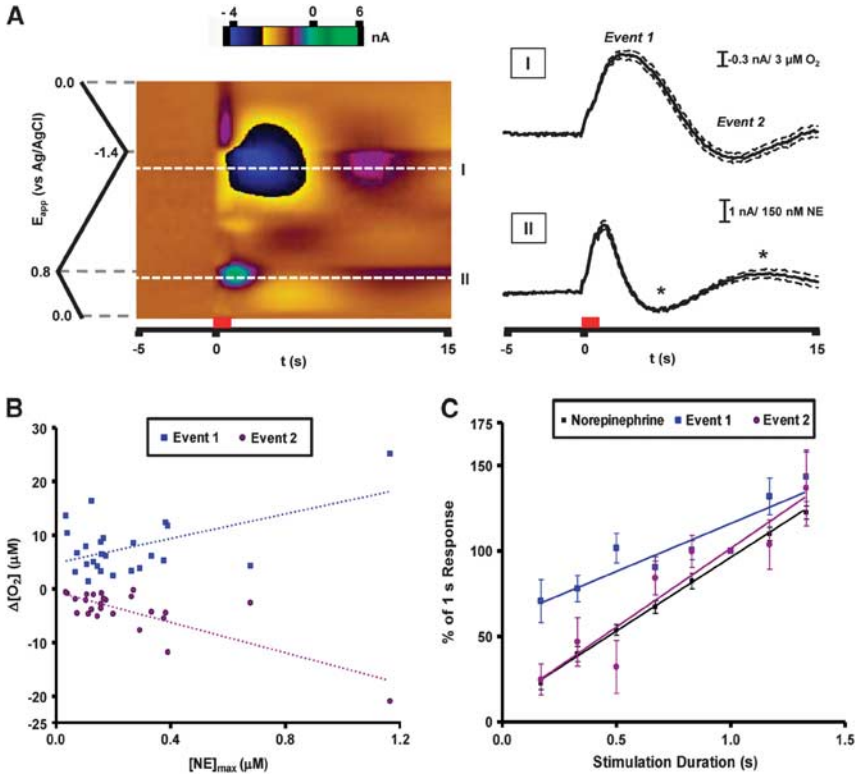

Figure 2. Predominant O_2 response recorded in the ventral bed nucleus of the stria terminalis with electrical stimulation of the ventral noradrenergic bundle. (**A**) Representative data averaged from 10 consecutive stimulations in a single animal. Current at all applied potentials is visualized in a false color display (left) with the stimulation time denoted by the red bar. Extracellular O_2 is monitored at its reduction potential (-1.35 V, I). Current extracted from this potential reveals a biphasic O_2 response after electrical stimulation. Norepinephrine release is simultaneously measured at its oxidation potential ($+0.75$ V, II) and is visible shortly after the stimulation onset. Changes in extracellular pH also generate current at this potential later in the recording (asterisks). Dashed lines indicate the s.e.m. for these measurements. (**B**) Magnitude of the O_2 response compared with stimulated norepinephrine release across multiple animals ($n=25$). Both O_2 events showed linear responses to the concentration of evoked norepinephrine (event 1: 11.46 ± 3.90 μmol/L O_2/μmol/L NE, $r^2=0.27$; event 2: -14.20 ± 2.37 μmol/L O_2/μmol/L NE, $r^2=0.61$). (**C**) Average peak amplitudes for norepinephrine and O_2 as a function of stimulation pulse number ($n=5$, 10 to 80 pulses). Each data set is normalized to the 60 pulse response. Responses for O_2 (event 1: $r^2=0.849$; event 2: $r^2=0.895$) and norepinephrine ($r^2=0.997$) were linear within this pulse range.

Table 1. Average responses to ventral noradrenergic bundle stimulation

Group	*Norepinephrine*		*Event 1*		*Event 2*	
	$[NE]_{max}$ (μmol/L)	t_{max} (s)	$[O_2]_{max}$ (μmol/L)	t_{max} (s)	$[O_2]_{max}$ (μmol/L)	t_{max} (s)
Control	0.22 ± 0.04	1.9 ± 0.1	6.98 ± 0.93	2.7 ± 0.1	-3.98 ± 0.74	9.6 ± 0.2
DSP-4	0.24 ± 0.10	2.0 ± 0.1	6.50 ± 1.95	3.2 ± 0.5	-5.59 ± 1.27	10.6 ± 1.3

No statistical difference between control and DSP-4 treated animals, *t*-test with Welch's correction for unequal variance. Control $n=25$, DSP-4 treatment $n=5$.

systemic administration of adrenergic drugs and anesthesia can influence cardiorespiratory function, we also monitored heart rate and breathing rate after their systemic application (Supplementary Figure 6). Urethane had no effect on breathing rate but did suppress heart rate. The adrenergic drugs exerted minor effects on these parameters.

Pharmacology of the VNB-stimulated O_2 changes is summarized in Figure 3. The average baseline peak amplitudes of event 1 and 2 were taken as 100% and compared with post-drug values. Vehicle treatments (local or systemic) did not affect either event. Event 1 was only affected by systemic administration of terazosin, an α_1-antagonist, and local administration of L-NAME, a NO synthesis inhibitor. Event 2 was attenuated by local administration of 1-aminobenzotriazole, a cytochrome P450/20-HETE synthesis inhibitor. Interestingly, event 2 was also sensitive to local blockade of all adrenoceptor types, decreasing with administration of terazosin, idazoxan (α_2 antagonist), and propranolol (β-antagonist). Systemic administration of the adrenergic drugs produced matching results except for terazosin, probably because of its competing effect on event 1. To assess the effect of increasing stimulated norepinephrine release without influencing presynaptic α_2 activity, which controls autoinhibition of release, the norepinephrine transporter blocker desipramine was administered. Desipramine increased the magnitude of event 2, although the effect was only significant with systemic administration. As this result opposes the effects of α_2 inhibition, the effect of idazoxan on the O_2 response is most likely due to post-synaptic actions, not increased norepinephrine overflow.

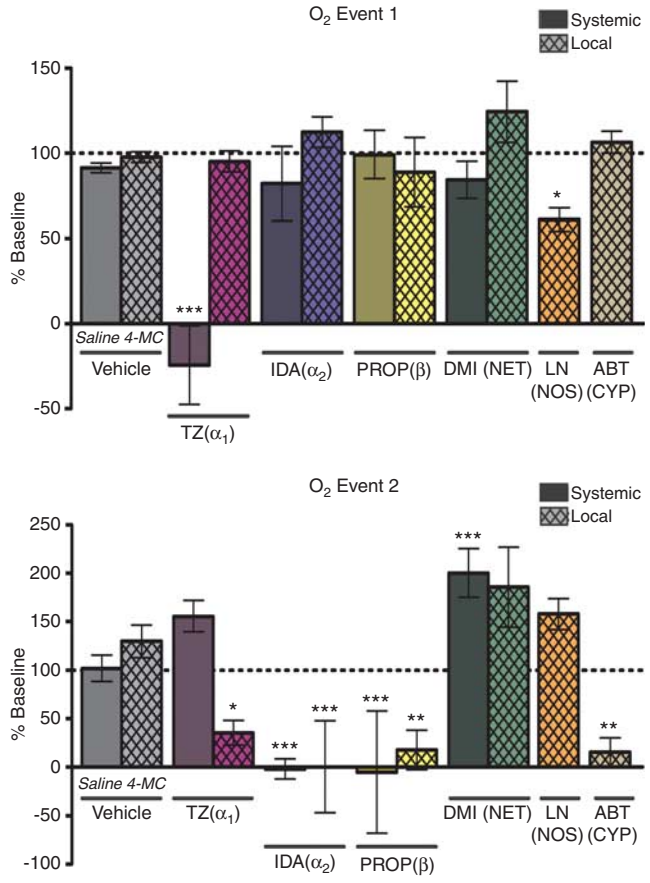

Figure 3. Pharmacology of the ventral noradrenergic bundle-stimulated O_2 response recorded in the ventral bed nucleus of the stria terminalis. The substrate inhibited is indicated underneath the data columns. Systemic drug administration (solid) was performed through intraperitoneal injection. Local drug administration (cross-hatch) was accomplished through iontophoretic ejection. $n = 5$ for all groups except saline ($n = 25$). Data are reported as a percentage of baseline. Significance was determined by a one-way analysis of variance with a Bonferroni *post hoc* test comparing drug with its vehicle control (saline or 4-MC). $^*P < 0.05$, $^{**}P < 0.01$, $^{***}P < 0.001$. ABT, 1-aminobenzotriazole; CYP, cytochrome P450; DMI, desipramine; IDA, idazoxan; 4-MC, 4-methylcatechol; LN, L-NAME; NET, norepinephrine transporter; NOS, nitric oxide synthase; PROP, propranolol; TZ, terazosin.

Local Iontophoresis of Norepinephrine

To preclude the confounding effects of co-release with electrical stimulation, we used iontophoresis to directly apply norepinephrine at the site of the recording electrode within the vBNST (Figure 4). Iontophoresis of 4-methylcatechol, the electroactive marker for the drug solutions, did not produce current changes at the reduction potential for O_2 (Figure 4B), confirming the absence of vehicle effects. Administration of norepinephrine (1 second ejections), however, induced O_2 fluctuations that mimicked those following VNB stimulation (Figure 4C). When this experiment was repeated in brain slice preparations, no O_2 response was observed with iontophoresis of norepinephrine (Figure 4D, $n = 4$ animals, two slices from each animal).

Using the carbon fiber microelectrode to monitor iontophoretic ejections, a range of norepinephrine concentrations (1 second ejections) were delivered at each recording location. Both the increase (event 1) and decrease (event 2) phases of the O_2 response showed dose dependence to the amount of norepinephrine ejected (Figure 4E). Neither event saturated within the range of norepinephrine concentrations assayed (50 nmol/L to 15 μmol/L). The absolute ratio of event 1 to event 2 (0.81 ± 0.07, $n = 12$ animals, 27 concentrations) was lower than for electrical stimulation (4.87 ± 1.52, $n = 25$ animals). As with electrical stimulation, the peak time of event 1 closely tracked the ejection, while the peak time of event 2 was more delayed with increased norepinephrine output ($t_p = 11.2$ to 23.2 seconds after ejection, Supplementary Figure 7). There was some variability in the O_2 response between animals. In a few locations (16.7%) only event 1 was evoked, while in others (16.7%) only event 2 was produced.

Local response pharmacology was investigated by using the remaining iontophoresis barrels to apply norepinephrine receptor antagonists. Event 1 was sensitive to β-receptor antagonism by propranolol ($P < 0.05$, $n = 5$). Similar to the VNB-stimulated response, event 2 could be attenuated by inhibition of all receptor types ($P < 0.01$ for terazosin, $n = 3$, idazoxan, $n = 4$, and propranolol, $n = 5$, Figure 4F).

Local Iontophoresis of Selective Adrenoceptor Agonists

Methoxamine (α_1 agonist), clonidine (α_2 agonist), and isoproterenol (β-agonist) were delivered iontophoretically (1 second ejections, 1 to 15 μmol/L) to assess whether any portion of the O_2 response could be triggered by activation of a single adrenoceptor type. Example responses are provided in Figure 6. Agonism of α_1 and α_2 receptors induced transient O_2 decreases (Figures 5A and 5B). The timing and number of these decreases varied from trial-to-trial and across animals. In some animals, no response was apparent while in others, the response was oscillatory in nature. In contrast, the β-agonist isoproterenol produced a time-locked increase in extracellular O_2, which reached a maximum slightly after the ejection. This response was found in all vBNST locations assayed (Figure 5C). In many animals (63.6%), the O_2 increase was again followed by a transient decrease event (Figure 5C, right). Compared with the responses observed after iontophoresis of norepinephrine, the absolute ratio of event 1 to event 2 was much larger for isoproterenol (5.40 ± 0.87, $n = 11$ animals, 22 concentrations).

DISCUSSION

A vast collection of literature supports a role for noradrenergic neurotransmission in functional hyperemia.[10,32] The simultaneous detection of norepinephrine and O_2 with high temporal resolution permitted us to directly probe local noradrenergic mechanisms. Moreover, the micrometer dimensions of the carbon fiber electrode allowed us to target the vBNST, a deep brain region innervated by non-coerulean norepinephrine neurons. We found both electrically evoked and iontophoretically applied norepinephrine induced similar O_2 responses in this region. Norepinephrine was found to have opposing roles in these responses. The initial O_2 increase involved a β-component, but principally originated from release of other substances including NO. At later times, synergistic activation of α- and β-adrenoceptors induced an O_2 decrease. These results reveal the complex control of O_2 levels by norepinephrine in the vBNST that originates from the multicellular locations of its receptors and their modulation of other chemical messengers (Figure 6). In a slice preparation, where blood flow is absent but metabolic activity can be evoked, increasing O_2 consumption, electrical stimulation caused prolonged O_2 decreases. O_2 changes were not detectable after iontophoresis of norepinephrine in slices. These results support a hyperemic origin of the *in vivo* O_2 responses.

The vasoactions of central norepinephrine are usually attributed to LC neurons.[5,8,10,15,32] In our preparation, the placement of the stimulating electrode activates other noradrenergic neurons, including the nucleus of the solitary tract and A1 cell groups. However, electrical stimulations are non-specific, and may result in

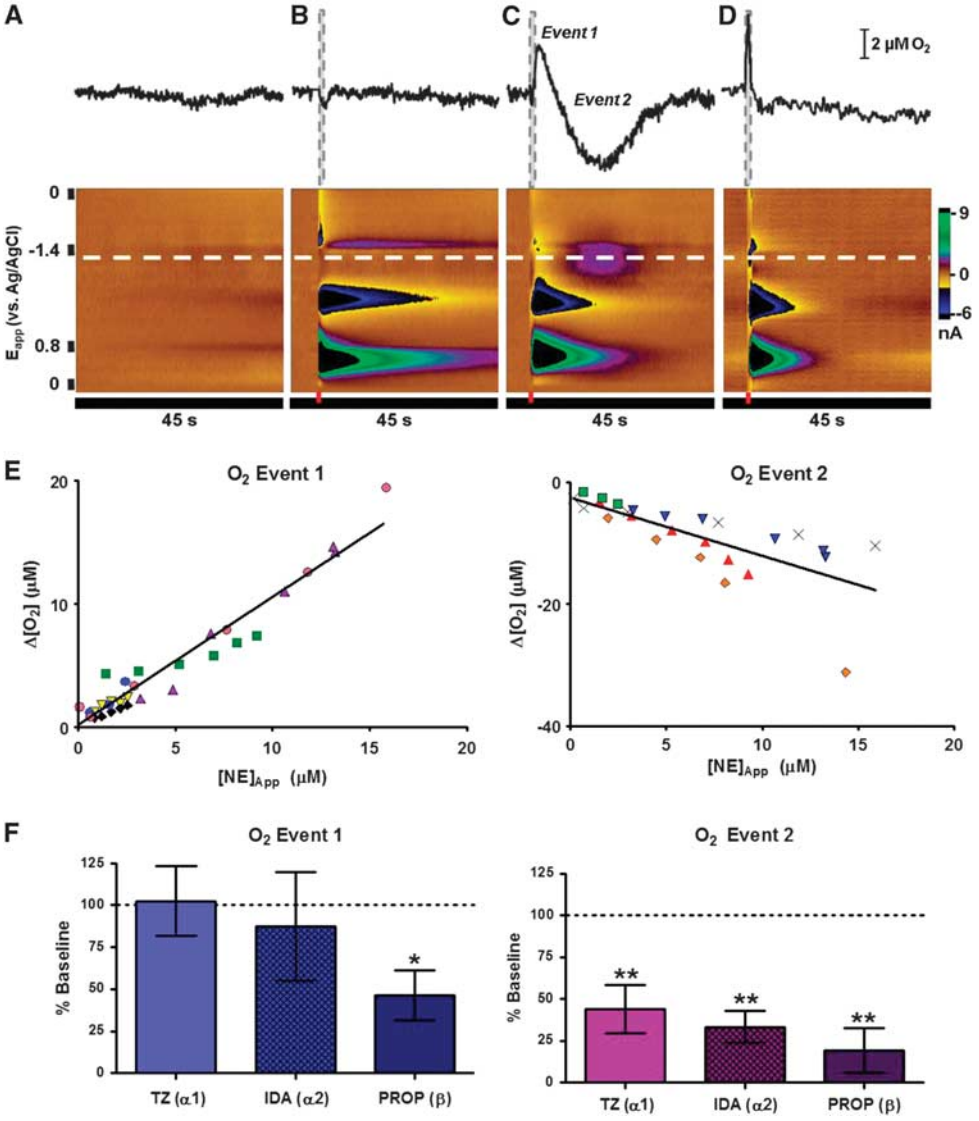

Figure 4. O_2 changes induced by direct delivery of norepinephrine with iontophoresis. (**A**–**D**) Example responses from a single recording location. Introduction of 4 μmol/L norepinephrine *in vivo* (**C**) evokes a biphasic O_2 response that is not an artifact of natural activity (**A**) or vehicle (**B**, ejection of 4 μmol/L 4-methylcatechol). Iontophoresis of similar norepinephrine concentrations in the ventral bed nucleus of the stria terminalis in a brain slice does not induce O_2 changes (**D**, 4 μmol/L ejection). The recording potential for O_2 is indicated by the white dashed lines. Ejection times (1 second in duration) are denoted by the red and gray dashed bars. (**E**) Magnitude of O_2 changes compared with the concentration of norepinephrine measured at the electrode. Data collected from the same recording location (average of 6 to 10 stimulations) are coded by point color and shape. (**F**) Effect of iontophoresed adrenoceptor antagonists terazosin (TZ, $n = 3$), idazoxan (IDA, $n = 4$) and propranolol (PROP, $n = 5$)) on the O_2 response. Significance was determined by a Dunnett's *post hoc* test after a one-way analysis of variance. *$P < 0.05$, **$P < 0.01$. IDA, idazoxan; PROP, propranolol; TZ, terazosin.

off-target depolarizations. As the vBNST receives a small percentage of its noradrenergic innervation from the LC,[33] and electrical stimulation of the LC elicits release,[27] we needed to assess coerulean influence on O_2 dynamics in the vBNST. To achieve this, we lesioned LC fibers with a selective neurotoxin. Electrically evoked O_2 responses were unchanged after LC lesioning, suggesting the noradrenergic contribution arose from the nucleus of the solitary tract and A1 innervation, and not indirect LC stimulation. As DSP-4 does affect hemodynamics in cortical regions,[15,32] it is unlikely that our results are skewed by compensatory mechanisms that evolved between administration of the neurotoxin and the recordings. To our knowledge, this data is the first to implicate norepinephrine release from these medullary cell populations in functional hyperemia.

Variation in O_2 fluctuations was witnessed across animals, which was likely due in part to the ability of our sensor to capture neurovascular heterogeneity that exists at submillimeter scales within the vBNST. However, in the majority of animals, electrical stimulation evoked an O_2 increase, which closely resembled the temporal dynamics of norepinephrine release and uptake, followed by an O_2 decrease. We observed similar effects after iontophoretic application of norepinephrine, affirming that norepinephrine's effects were mediated in the local terminal field and not by activity in other brain regions. In both stimulation and iontophoresis paradigms, the magnitude of each O_2 event increased with the norepinephrine output, but did not saturate within the concentration ranges assayed. Taken together, these data support the notion that norepinephrine release affects a

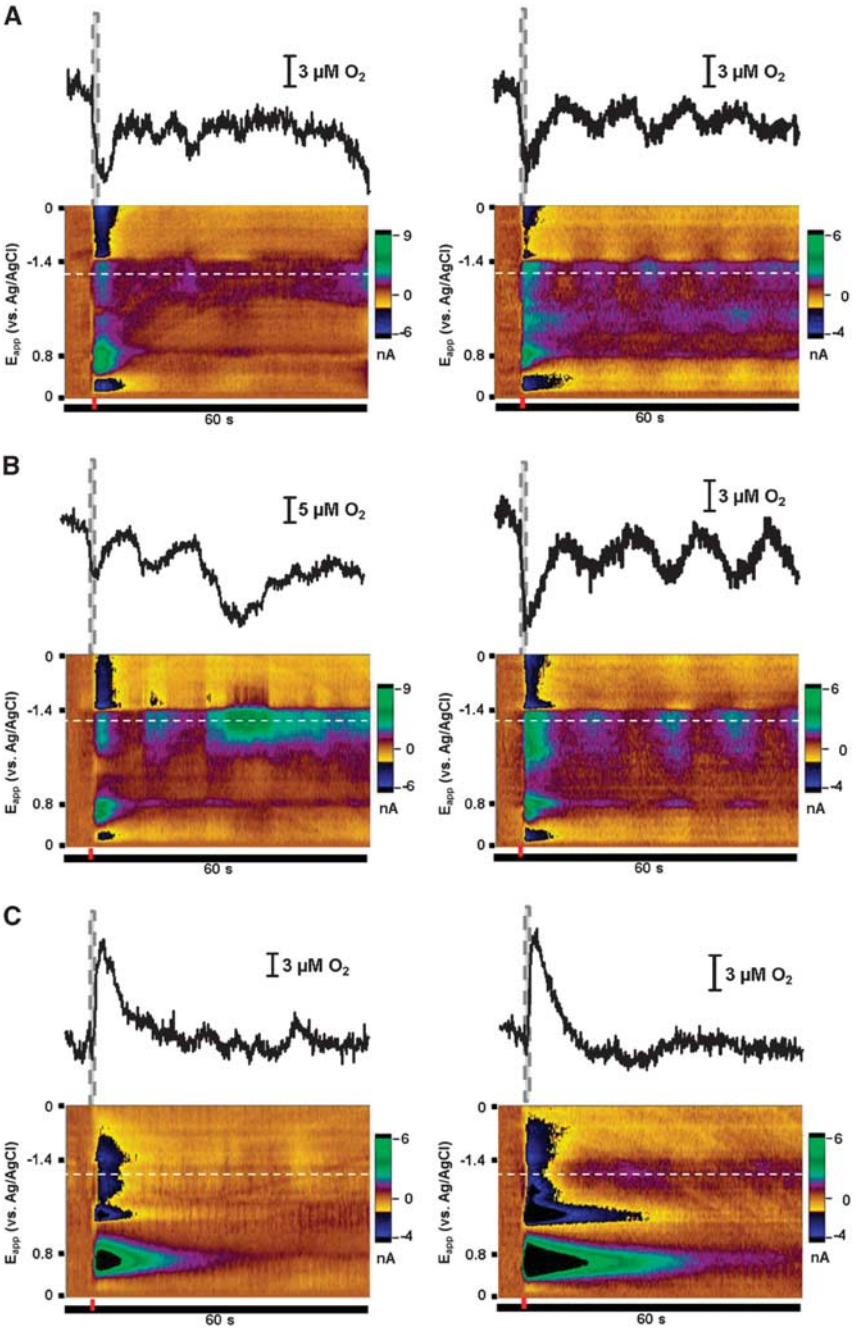

Figure 5. O_2 changes induced by local delivery of adrenoceptor agonists with iontophoresis. Example responses to methoxamine (α_1 agonist, **A**), clonidine (α_2 agonist, **B**), and isoproterenol (non-selective β-agonist, panel **C**) are shown for different recording locations. The recording potential for O_2 is indicated by the whited dashed lines. Ejection times (1 second in duration) are denoted by the gray dashed bars and the red bars.

vascular area proportional to presynaptic activity, consistent with restricted volume neurotransmission.

Adrenoceptors are expressed in neurons, astrocytes, endothelial cells, pericytes, and smooth muscle[7,34]—the major constituents of the neurovascular system. Indeed, 8% of noradrenergic terminals in the cortex are located in the perivascular space, and are not proximal to neuronal targets.[5] Through receptor activation, norepinephrine likely influences the concerted actions of these components to support metabolic needs. The data here demonstrate that each event of the O_2 response had distinct signaling pathways. In the vBNST, we found event 1 to be partially dependent on local β-receptor activity. When evoked by direct application of norepinephrine, event 1 could be blocked by the non-selective β-antagonist, propranolol, and was reproduced by the β-agonist, isoproterenol. This pharmacology is consistent with the well-documented dilatory effect of β-receptors on vascular smooth muscle. As β-receptors are expressed on rat cerebral microvessels,[35] a transient surge of norepinephrine in the vBNST may directly induce local vasodilation, thereby increasing the inflow of O_2-rich blood and giving rise to event 1. Indirect mechanisms cannot be discounted, however. Stimulation of β-receptors in this region may influence local cell activity and, in turn, the release of vasodilators dependent on this activity. A study by Winder and coworkers[36] found β-pharmacology to have no

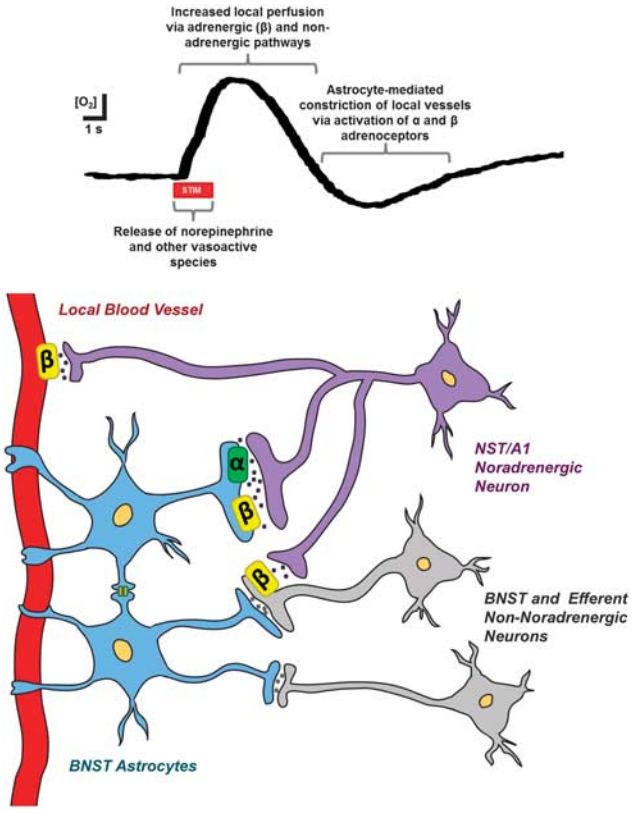

Figure 6. Proposed mechanism underlying the O_2 responses recorded after electrical stimulation of the ventral noradrenergic bundle (VNB). Temporal (upper) and spatial (lower) models are provided. Stimulation of the VNB induces norepinephrine release from noradrenergic cells originating in the nucleus of the solitary tract (NST) and A1 cell groups. Non-noradrenergic cell populations coursing near the coordinates of the stimulating electrode are also excited, leading to simultaneous release of other neurotransmitters within the ventral bed nucleus of the stria terminalis (vBNST). This overflow of norepinephrine and other vasoactive neurotransmitters causes dilation of local microvessels and a subsequent influx of O_2. The noradrenergic contribution to this response is mediated through activation of β-adrenoceptors either indirectly, by modulating local cell activity, or directly, by relaxation of vascular smooth muscle. Local O_2 concentrations continue to rise shortly after the stimulation ceases. Thereafter, a signaling cascade initiated by the synergistic activation of adrenoceptors on astrocytes results in the release of secondary messengers from astrocytic endfeet. These messengers act upon vessels to cause their constriction, and in turn, provide an active termination of the hyperemic response. As a result, O_2 levels transiently decrease before returning to baseline concentrations.

effect on glutamatergic transmission in the vBNST. Therefore, if event 1 is produced by an indirect noradrenergic mechanism, it is unlikely due to the alteration of glutamatergic activity.

In apparent contradiction, electrically evoked O_2 changes only responded to peripheral blockade of α_1 receptors. Adrenergic α_1 receptors are known to constrict superficial cerebral arteries and arterioles in the rat,[32] and their dilation may blunt the redirection of blood flow to the BNST. Consistent with a remote location of α_1 modulation, Event 1 was not produced or inhibited by local application of α_1 pharmacology. While iontophoresis of the β-agonist produced an O_2 increase, its contribution to event 1 appears to be masked when evoked through electrical stimulation. This is likely because of the actions of co-released neuromodulators initiated by non-selective neuronal activation. Ventral noradrenergic bundle stimulation also depolarizes neurons in the ventral tegmental area/substantia nigra that could release vasodilators such as acetylcholine,[25] which cannot be detected by our technique. Consistent with this view, we found that event 1 could be attenuated by inhibiting the synthesis of NO locally in the vBNST.

During the second O_2 event, concentrations transiently decreased below baseline levels. This observed decrease required local activation of both α- and β-adrenoceptors. Although it is not possible to comment on their relative contributions, inhibition of each adrenoceptor attenuated the decrease. Interestingly, when selective agonists were applied, only activation of β-receptors with isoproterenol produced a time-locked response that resembled event 2. In contrast, iontophoresis of the α-agonists methoxamine and clonidine was followed by O_2 decrease events. It is possible that α_1 and α_2 receptors, which have higher affinity than β-types, are partially occupied by tonic concentrations within the norepinephrine-rich vBNST. Baseline α-activity therefore may be enough to permit the O_2 response when low affinity β-receptors are stimulated. As expected in this scenario, the ratio of event 1 to 2 is much larger for isoproterenol in comparison with norepinephrine, which binds to both α- and β-receptor types.

Although reported less frequently, cerebral O_2 decreases have been cited in the literature.[37] For a healthy organism, it is unlikely that these occurrences are due to an imbalance of metabolic demand. More accepted are the theories that O_2 decreases arise from reduced blood flow because of either 'vascular steal' from other activated brain regions or local neuronal inactivation. The timing and pharmacology of event 2 in our study supports the possibility of a constriction-mediated termination of the initial O_2 increase, a function that has been associated with noradrenergic signaling in the somatosensory cortex.[32] Norepinephrine-mediated constrictions are canonically produced by vascular α-adrenoceptor activation. However, the β-sensitivity of event 2 and the temporal delay of its onset after norepinephrine clearance indicate that the O_2 decrease arises from noradrenergic activation of other chemical messengers that subsequently act at the vascular wall.

Astrocytes present a potential intermediary. These glial cells express all adrenoceptor types and are well documented to respond to norepinephrine.[7,38] Of its many effects, noradrenergic stimulation is reported to induce intracellular Ca^{2+} waves, which can propagate over entire astrocyte populations. One study demonstrated that norepinephrine-evoked Ca^{2+} events are followed by constriction of nearby vessels, theorized to be due to generation of 20-HETE.[39] In agreement with their observations, the magnitude of event 2 was reduced with 1-aminobenzotriazole, which blocks formation of 20-HETE through inhibition of cytochrome P450. In addition, we observed transient decreases in O_2 with α-adrenoceptor activation that were often oscillatory in nature, much like astrocyte Ca^{2+} fluctuations. Supporting the additional involvement of β-signaling in event 2, both α- and β-receptors can stimulate astrocyte Ca^{2+} responses *in vivo*,[40,41] and synergistic activation of these receptors potentiates Ca^{2+} responses *in vitro*.[42] Although it is not possible to dismiss indirect vascular effects through altered neuronal activity,[36] the reported effects of norepinephrine on astrocytes are overall consistent with the temporal and pharmacological characteristics of event 2.

In summary, we have established a role for brainstem norepinephrine neurons in the control of extracellular O_2 in a terminal region. When activated, these cells increased norepinephrine overflow in the vBNST, locally triggering a biphasic O_2 response. This response was absent in a preparation that lacked CBF and had distinct receptor mechanisms. The initial increase involved a small β-receptor component and was also due to NO formation. The subsequent decrease was induced by the synergistic actions of α-and β-receptor types. The delayed

temporal characteristics of this decrease indicate that adrenergic activation induced a chemical cascade resulting in the formation of 20-HETE, a known vasoconstrictor. Oscillatory O_2 responses to selective agonists suggest astrocytes may mediate this cascade. These data support the view that norepinephrine is one of many substances that can match energy demands and supply in the brain.

DISCLOSURE/CONFLICT OF INTEREST

The authors declare no conflict of interest.

ACKNOWLEDGMENTS

The authors thank V Gukassyan for technical assistance and the UNC Neuroscience Center Microscopy Core (P30 NS045892).

REFERENCES

1 Cauli B, Hamel E. Revisiting the role of neurons in neurovascular coupling. *Front Neuroenergetics* 2010; **2**: 9.
2 Baker WB, Sun Z, Hiraki T, Putt ME, Durduran T, Reivich M *et al.* Neurovascular coupling varies with level of global cerebral ischemia in a rat model. *J Cereb Blood Flow Metab* 2013; **33**: 97–105.
3 Bell RD, Zlokovic BV. Neurovascular mechanisms and blood-brain barrier disorder in Alzheimer's disease. *Acta Neuropathol* 2009; **118**: 103–113.
4 Latsari M, Dori I, Antonopoulos J, Chiotelli M, Dinopoulos A. Noradrenergic innervation of the developing and mature visual and motor cortex of the rat brain: a light and electron microscopic immunocytochemical analysis. *J Comp Neurol* 2002; **445**: 145–158.
5 Cohen Z, Molinatti G, Hamel E. Astroglial and vascular interactions of noradrenaline terminals in the rat cerebral cortex. *J Cereb Blood Flow Metab* 1997; **17**: 894–904.
6 Aoki C, Venkatesan C, Go CG, Forman R, Kurose H. Cellular and subcellular sites for noradrenergic action in the monkey dorsolateral prefrontal cortex as revealed by the immunocytochemical localization of noradrenergic receptors and axons. *Cereb Cortex* 1998; **8**: 269–277.
7 Hertz L, Lovatt D, Goldman SA, Nedergaard M. Adrenoceptors in brain: cellular gene expression and effects on astrocytic metabolism and $[Ca^{2+}]i$. *Neurochem Int* 2010; **57**: 411–420.
8 Kalaria RN, Stockmeier CA, Harik SI. Brain microvessels are innervated by locus ceruleus noradrenergic neurons. *Neurosci Lett* 1989; **97**: 203–208.
9 Obel LF, Andersen KM, Bak LK, Schousboe A, Waagepetersen HS. Effects of adrenergic agents on intracellular Ca^{2+} homeostasis and metabolism of glucose in astrocytes with an emphasis on pyruvate carboxylation, oxidative decarboxylation and recycling: implications for glutamate neurotransmission and excitotoxicity. *Neurotox Res* 2012; **21**: 405–417.
10 Raichle ME, Hartman BK, Eichling JO, Sharpe LG. Central noradrenergic regulation of cerebral blood flow and vascular permeability. *Proc Natl Acad Sci USA* 1975; **72**: 3726–3730.
11 Muyderman H, Hansson E, Nilsson M. Adrenoceptor-induced changes of intracellular K^+ and Ca^{2+} in astrocytes and neurons in rat cortical primary cultures. *Neurosci Lett* 1997; **238**: 33–36.
12 Gibbs ME, Hutchinson D, Hertz L. Astrocytic involvement in learning and memory consolidation. *Neurosci Biobehav Rev* 2008; **32**: 927–944.
13 Alexander GM, Grothusen JR, Gordon SW, Schwartzman RJ. Intracerebral microdialysis study of glutamate reuptake in awake, behaving rats. *Brain Res* 1997; **766**: 1–10.
14 Goadsby PJ, Duckworth JW. Low frequency stimulation of the locus coeruleus reduces regional cerebral blood flow in the spinalized cat. *Brain Res* 1989; **476**: 71–77.
15 Toussay X, Basu K, Lacoste B, Hamel E. Locus coeruleus stimulation recruits a broad cortical neuronal network and increases cortical perfusion. *J Neurosci* 2013; **33**: 3390–3401.
16 Dumont EC. What is the bed nucleus of the stria terminalis? *Prog Neuropsychopharmacol Biol Psychiatry* 2009; **33**: 1289–1290.
17 Kilts CD, Anderson CM. The simultaneous quantification of dopamine, norepinephrine and epinephrine in micropunched rat brain nuclei by on-line trace enrichment HPLC with electrochemical detection: distribution of catecholamines in the limbic system. *Neurochem Int* 1986; **9**: 437–445.
18 Forray MI, Gysling K. Role of noradrenergic projections to the bed nucleus of the stria terminalis in the regulation of the hypothalamic-pituitary-adrenal axis. *Brain Res Brain Res Rev* 2004; **47**: 145–160.
19 Swanson LW, Connelly MA, Hartman BK. Ultrastructural evidence for central monoaminergic innervation of blood vessels in the paraventricular nucleus of the hypothalamus. *Brain Res* 1977; **136**: 166–173.
20 Maeda M, Duelli R, Schrock H, Kuschinsky W. Autoradiographic determination of local cerebral blood flow and local cerebral glucose utilization during chemical stimulation of the nucleus tractus solitarii of anesthetized rats. *J Auton Nerv Syst* 1998; **69**: 132–140.
21 Cahill PS, Walker QD, Finnegan JM, Mickelson GE, Travis ER, Wightman RM. Microelectrodes for the measurement of catecholamines in biological systems. *Anal Chem* 1996; **68**: 3180–3186.
22 Herr NR, Kile BM, Carelli RM, Wightman RM. Electroosmotic flow and its contribution to iontophoretic delivery. *Anal Chem* 2008; **80**: 8635–8641.
23 Bucher ES, Brooks K, Verber MD, Keithley RB, Owesson-White C, Carroll S *et al.* Flexible software platform for fast-scan cyclic voltammetry data acquisition and analysis. *Anal Chem* 2013; **85**: 10344–10353.
24 Heien ML, Phillips PE, Stuber GD, Seipel AT, Wightman RM. Overoxidation of carbon-fiber microelectrodes enhances dopamine adsorption and increases sensitivity. *Analyst* 2003; **128**: 1413–1419.
25 Venton BJ, Michael DJ, Wightman RM. Correlation of local changes in extracellular oxygen and pH that accompany dopaminergic terminal activity in the rat caudate-putamen. *J Neurochem* 2003; **84**: 373–381.
26 Keithley RB, Heien ML, Wightman RM. Multivariate concentration determination using principal component regression with residual analysis. *Trends Analyt Chem* 2009; **28**: 1127–1136.
27 Park J, Kile BM, Wightman RM. *In vivo* voltammetric monitoring of norepinephrine release in the rat ventral bed nucleus of the stria terminalis and anteroventral thalamic nucleus. *Eur J Neurosci* 2009; **30**: 2121–2133.
28 Park J, Takmakov P, Wightman RM. *In vivo* comparison of norepinephrine and dopamine release in rat brain by simultaneous measurements with fast-scan cyclic voltammetry. *J Neurochem* 2011; **119**: 932–944.
29 Fritschy JM, Grzanna R. Immunohistochemical analysis of the neurotoxic effects of DSP-4 identifies two populations of noradrenergic axon terminals. *Neuroscience* 1989; **30**: 181–197.
30 Hartig W, Reichenbach A, Voigt C, Boltze J, Bulavina L, Schuhmann MU *et al.* Triple fluorescence labelling of neuronal, glial and vascular markers revealing pathological alterations in various animal models. *J Chem Neuroanat* 2009; **37**: 128–138.
31 Takmakov P, Zachek MK, Keithley RB, Bucher ES, McCarty GS, Wightman RM. Characterization of local pH changes in brain using fast-scan cyclic voltammetry with carbon microelectrodes. *Anal Chem* 2010; **82**: 9892–9900.
32 Bekar LK, Wei HS, Nedergaard M. The locus coeruleus-norepinephrine network optimizes coupling of cerebral blood volume with oxygen demand. *J Cereb Blood Flow Metab* 2012; **32**: 2135–2145.
33 McNaughton N, Mason ST. The neuropsychology and neuropharmacology of the dorsal ascending noradrenergic bundle--a review. *Prog Neurobiol* 1980; **14**: 157–219.
34 Elfont RM, Sundaresan PR, Sladek CD. Adrenergic receptors on cerebral microvessels: pericyte contribution. *Am J Physiol* 1989; **256**: R224–R230.
35 Kobayashi H, Maoret T, Ferrante M, Spano P, Trabucchi M. Subtypes of β-adrenergic receptors in rat cerebral microvessels. *Brain Res* 1981; **220**: 194–198.
36 Egli RE, Kash TL, Choo K, Savchenko V, Matthews RT, Blakely RD *et al.* Norepinephrine modulates glutamatergic transmission in the bed nucleus of the stria terminalis. *Neuropsychopharmacology* 2004; **30**: 657–668.
37 Wade AR. The negative BOLD signal unmasked. *Neuron* 2002; **36**: 993–995.
38 Stone EA, Ariano MA. Are glial cells targets of the central noradrenergic system? A review of the evidence. *Brain Res Brain Res Rev* 1989; **14**: 297–309.
39 Mulligan SJ, MacVicar BA. Calcium transients in astrocyte endfeet cause cerebrovascular constrictions. *Nature* 2004; **431**: 195–199.
40 Bekar LK, He W, Nedergaard M. Locus coeruleus alpha-adrenergic-mediated activation of cortical astrocytes in vivo. *Cereb Cortex* 2008; **18**: 2789–2795.
41 Ding F, O'Donnell J, Thrane AS, Zeppenfeld D, Kang H, Xie L *et al.* α1-Adrenergic receptors mediate coordinated Ca^{2+} signaling of cortical astrocytes in awake, behaving mice. *Cell Calcium* 2013; **54**: 387–394.
42 Espallergues J, Solovieva O, Técher V, Bauer K, Alonso G, Vincent A *et al.* Synergistic activation of astrocytes by ATP and norepinephrine in the rat supraoptic nucleus. *Neuroscience* 2007; **148**: 712–723.

Supplementary Information accompanies the paper on the Journal of Cerebral Blood Flow & Metabolism website (http://www.nature.com/jcbfm)